

Auto Reconfigurable Patch Antenna for Biomedical Single Channel Multi-Frequency Microwave Radiometry Applications

Chris D. Nikolopoulos*, Anargyros T. Baklezos, and Christos N. Capsalis

Abstract—A small patch antenna is associated with passive (reactively loaded) elements (varactors) in order to auto adjust the resonant frequency in a single-channel multi-frequency configuration appropriate for biomedical applications. As a supplementary study of the authors in the field of detection of temperature abnormalities in human tissue phantom using microwave radiometry, this paper adds a contribution to frequency readjustment when a shift occur due to the fact that the human body is a complex and stratified dielectric object. The optimization of the array is performed using a Genetic Algorithm (GA) tool as a method of choice. The adjustment in the measurement frequency is performed by altering the values of the passive elements according to the shift needed.

1. INTRODUCTION

Microwave radiometry can respond better to thermal radiation emitted several centimeters below the skin because of its wavelength spectrum and lower frequency range (between 300 MHz and 300 GHz). It is undoubtful, as shown in the Figure 1, that in the microwave range the intensity is about 10 million (-70 dBW) times smaller than infrared radiation. Nevertheless, microwave radiation is less attenuated in tissue, thus is suitable for measuring the temperature subcutaneously. By using microwave radiometry, the power level of thermal radiation from a tissue region can be captured. Provided that anatomical information of the region is known, then this information can be used with the radiometer power measurements to detect temperature anomalies in the tissue.

The antenna should guarantee proper transmission or reception of electromagnetic signals, as any mistakes or faults at this stage greatly affect the effectiveness of the whole system. The requirements and, accordingly, the specifications of the antennas are driven by the numerous applications arising, yielding a wide variety of antenna design types.

When referring to antenna parameters, such as impedance, bandwidth and efficiency, the reference corresponds to those defined for the antenna located in free space. In biomedical radiometric sensing the antennas of the radiometer are used in environments comprising the free space and lossy medium, which is typically human tissue. Thus, it is important to discuss parameters that describe wave behavior in lossy medium.

Several studies have been conducted indicating that the dielectric properties of various biological tissues vary considerably depending on the water content. A key measurement parameter of microwave properties is the dielectric constant or permittivity, which is directly related to water content. The permittivity explains the material loss characteristics and ability to store energy when the material is placed in an electric field [1]. Water molecules attempt to align themselves within an electric field, because of their polar nature. As a result, low water content tissues as bone and fat tend to present low permittivity, whilst high water content tissues, such as muscle, blood, and internal organs, high permittivity [2–4]. The interaction of the lossy biological tissues with the microwave frequency may be

Received 19 February 2014, Accepted 16 March 2014, Scheduled 2 April 2014

* Corresponding author: Chris D. Nikolopoulos (chris.d.nikolopoulos@gmail.com).

The authors are with the Division of Information Transmission Systems and Material Technology, School of Electrical and Computer Engineering, National Technical University of Athens, 9, Iroon Polytechniou Str., Zografou, Athens 15773, Greece.

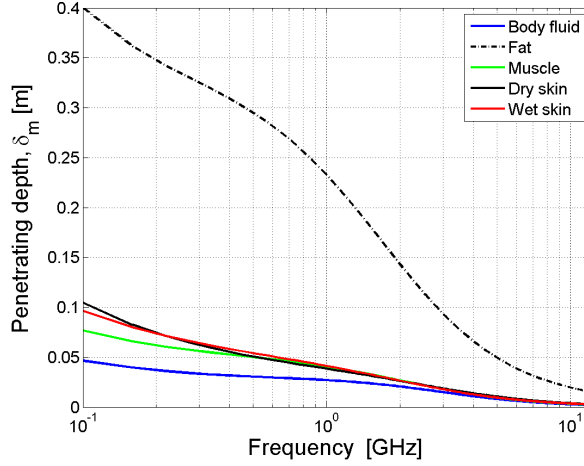


Figure 1. Skin depth versus frequency for some body-materials.

described by complex permittivity, ε^* , which is a complex quantity consisting of two separate parameters ε' and ε'' , and expressed as:

$$\varepsilon^* = \varepsilon' - j\varepsilon'' \quad (1)$$

In the above equation, the real part dielectric constant ε' is a measure of the ability of the tissue to store energy from an external electric field, and is given by:

$$\varepsilon' = \varepsilon_r \varepsilon_0 \quad (2)$$

where ε_r is the dielectric constant of the material and ε_0 the permittivity of free space [5]. The imaginary part of loss factor indicates the energy amount that is converted into heat and dissipated, due to damping of the vibrating dipole moments. The Debye equation is often used to model the complex relative permittivity and its frequency dependency [6]:

$$\varepsilon(\omega) = \varepsilon_\infty + \frac{\varepsilon_s - \varepsilon_\infty}{1 + j\omega\tau_r} \quad (3)$$

where ε_s and ε_∞ are the low and high frequency limits of the dielectric constant, respectively. ω is the angular frequency of the applied field and τ_r the relaxation time. When splitting the above equation into real and imaginary parts, the following two equations arise:

$$\varepsilon'(\omega) = \varepsilon_\infty + \frac{\varepsilon_s - \varepsilon_\infty}{1 + \omega^2\tau_r^2} \quad \text{and} \quad \varepsilon''(\omega) = + \frac{(\varepsilon_s - \varepsilon_\infty)\omega\tau_r}{1 + \omega^2\tau_r^2} \quad (4)$$

Tissue materials are a composition of biological materials with different frequency dependence (dispersion) regions. The complexity of both structure and composition of the material is such that each region with dispersion may be broadened [7, 8], caused by the multiple contributions to the dispersion region. In order to empirically quantify this broadening, a new parameter is introduced, called distribution parameter α . Its use leads to an alternative to the Debye equation, the so-called Cole-Cole equation [9]:

$$\varepsilon(\omega) = \varepsilon_\infty + \frac{\varepsilon_s - \varepsilon_\infty}{1 + (j\omega\tau_r)^{1-\alpha}} \quad (5)$$

A multiple Cole-Cole dispersion can be expressed by generalizing this equation to:

$$\varepsilon(\omega) = \varepsilon_\infty + \sum_n \frac{\Delta\varepsilon_n}{1 + (j\omega\tau_{r,n})^{1-\alpha_n}} + \frac{\sigma_i}{j\omega\varepsilon_0} \quad (6)$$

where $\Delta\varepsilon = \varepsilon_s - \varepsilon_\infty$, and σ_i is the static ionic conductivity. With a proper choice of parameters relevant to each material, the latter equation can be used to model the dielectric properties over a given

frequency range. Debye relaxation equation can estimate the conductivity as the loss factor includes the effect of conductivity, in terms of:

$$\varepsilon''(\omega) = \sigma / \varepsilon_0 \omega \quad (7)$$

As a result, the conductivity value for a given frequency is represented by:

$$\sigma = \frac{\varepsilon_0(\varepsilon_s - \varepsilon_\infty)\omega^2\tau_r}{1 + \omega^2\tau_r^2} \quad (8)$$

The loss tangent is a parameter of a dielectric material that quantifies its inherent dissipation of electromagnetic energy. The term refers to the loss caused by the dissipation of the energy to the lossy medium and is expressed as

$$\tan \delta = \frac{\omega\varepsilon'' + \sigma}{\omega\varepsilon'} \quad (9)$$

where $\omega = 2\pi f$ is the angular frequency and σ is conductivity.

When the antenna is located close to human body, the effective wavelength deviates from the free space wavelength. This is typically observed as a shift of the antenna resonance frequency (this relevance depicted in Figure 2). The permittivity affects the antenna resonance frequency f_r as:

$$f_r = \frac{c}{\sqrt{\varepsilon_{eff}}\lambda} \quad (10)$$

where c is the velocity of light and λ the wavelength. Antenna reception depends on the distance between the antenna and the body, as well as the effective permittivity.

Another important parameter which is essential when studying electromagnetic propagation in a material is the skin depth, which is given by:

$$\delta_m = \frac{1}{\sqrt{\pi f \mu \sigma}} \quad (11)$$

where f is the frequency and μ the permeability of the material. The skin depth gives a measure of the average depth of penetration of the electromagnetic field. In low frequencies, the permittivity is relatively high, thus the conductivity is low, and the electromagnetic wave can propagate through the tissues without too much attenuation. At higher frequencies, the loss is increased, hence the skin depth decreases.

Microwave thermography, microwave hyperthermia and microwave tomographic systems, all rely on processes fundamentally determined by the high frequency electromagnetic properties of human tissues. As stated above, the vicinity to the human body introduces dielectric characteristics in front of an antenna which affects the resonant frequency (some MHz shift in central frequency) [10–12], which in turn affects the antenna input impedance. This leads finally to loss of matching, a fact that translates into additional losses in the radiometer system. Consequently, a number of recent works and studies are directed to reconfigurable solutions, so that matching is always achieved.

For the reason mentioned above we propose in this study an auto reconfigurable patch antenna which can auto adjust its resonant frequency depending on the dielectric properties of the medium. As described before and in case of a single channel measurement, the dielectric properties of the medium change (shift) the central frequency (the frequency in which we have matching the input impedance) of the channel, so if we have a common antenna system the measurement would not be accurate, and we use the reconfigurable concept of a previous work of the authors [13] in which a set of varactor diodes are used to change the resonant frequency on demand [14–16].

2. ARCHITECTURE OF THE PATCH ANTENNA

The structure under consideration is depicted in Figure 3. The only active element consists of a top plate connected with the ground plane through a three shorting strips (reactance loaded) and one feed wire. By altering the dimensions of the top plates, the height above the ground plane and the size of the ground plane, the structure with the best impedance matching at the frequency of operation (1800 MHz) and adequate bandwidth will be derived.

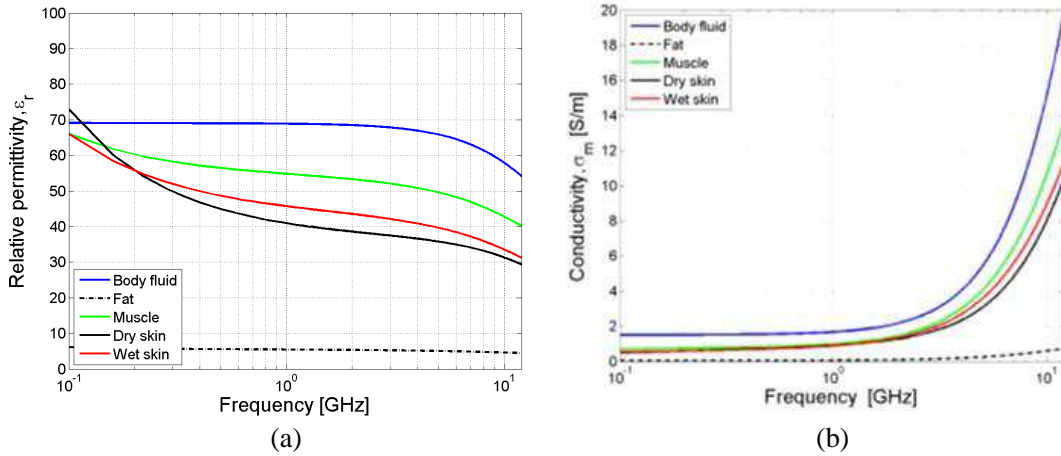


Figure 2. Relative permittivity versus frequency for some body materials, Conductivity versus frequency for some body materials.

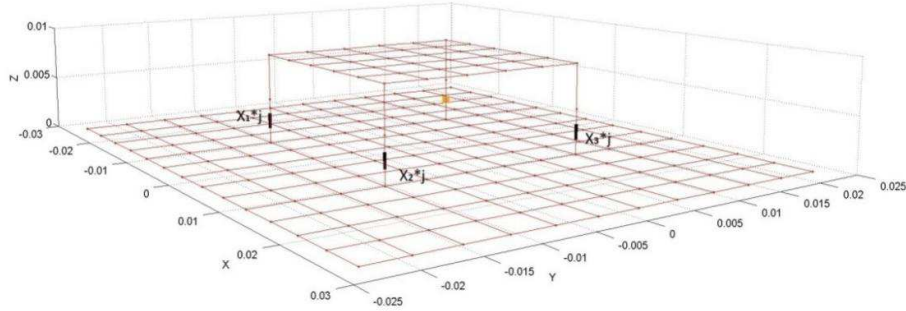


Figure 3. Implementation and analysis of the patch antenna using wire segments and the SNEC platform.

The structure is generated with the use of SuperNEC simulation software package, and its performance is optimized by utilizing the Genetic Algorithms (GA) approach. Using the same methodology as the previous work of the authors [13] a better antenna structure is achieved (dimensions $W: 0.046 \text{ m} \times L: 0.054 \text{ m} \times H: 0.0083 \text{ m}$) with an operative range between 1200 MHz–6650 MHz (depending on the values of the varactor diodes). A GA is capable of facing multi-variable problems, such as the design and synthesis of antennas, where a set of performance conditions (e.g., input impedance) should be satisfied.

The SNEC results were evaluated via the Finite Elements Method using Asoft HFSS 3D simulation software (High Frequency Structure Simulator — which offers a linear electromagnetic solution to the physical specified structure based on the finite elements analysis). In the design process depicted in Figure 4(a), we use copper as the assigned material for both the upper plates and ground plane. In addition, in the sorting strips we add varactor — simulated elements (we model the varactor as resistance + capacitance, for that reason a lumped RLC with proper characteristics was utilized to simulate the effects of the varactor diode, taking into account the resonant frequency of 1.8 GHz). Finally as a full port impedance, we use a resistance of 50 Ohms (to be consistent with the one selected in the SNEC implementation).

To add an auto reconfigurable performance in the antenna design, we propose a simple algorithm (Figure 6) which can affect the antenna performance with respect to the dielectric properties of the body in front of the patch. With a proper closed loop system, the antenna can scan appropriate range of frequencies (specific channel, e.g., frequency range 1500 MHz–1600 MHz) every 10 MHz, then measure the S_{11} parameter and compare with the previous measurement tuning in that way to the one with the

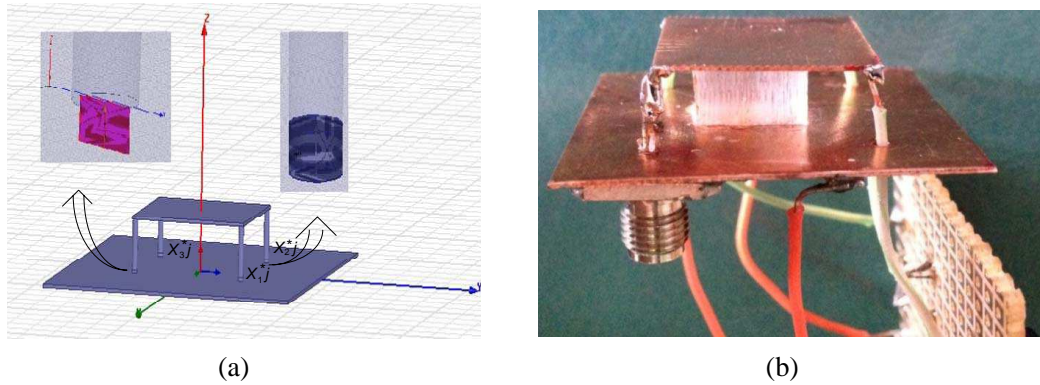


Figure 4. (a) The complete reconfigurable patch antenna layout using Ansoft HFSS 3D simulation software and (b) the antenna structure constructed with copper sheets.

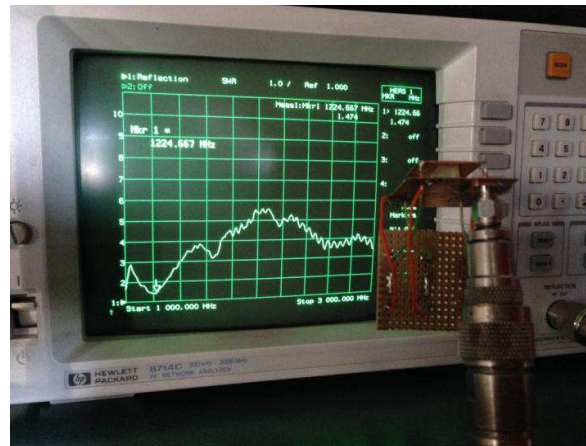


Figure 5. Measurement of the proposed antenna at 1250 MHz ($X_1 = -62$, $X_2 = -28$, $X_3 = -94$).

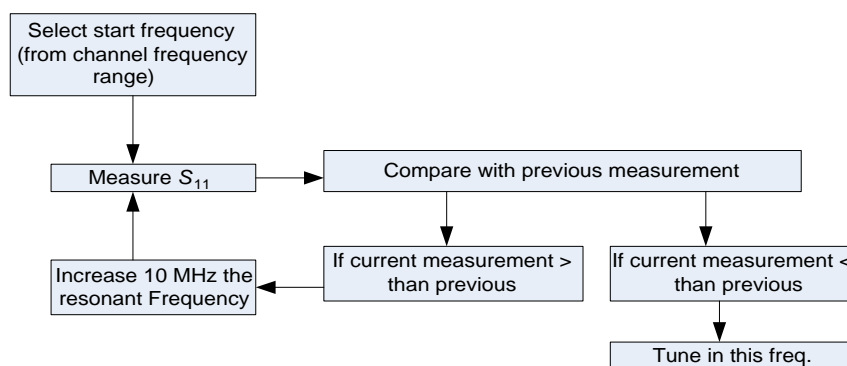


Figure 6. The proposed closed loop algorithm.

best value. So a quick scan should be performed every time the radiometer operates in a different channel (according to the dielectric properties of the human tissue and because the impedance matching would change, so a frequency shift will occur) to tune in the correct frequency. The implementation of this routine is performed with a simple microcontroller which can compare the values of S_{11} parameter and when find the best, from a database stored in a ram, would retrieve the values of the load reactance of the sorting strips (from a table like Table 2), and change the voltage of the varactor diodes accordingly.

3. OPTIMIZATION PROCEDURE OF THE PATCH ANTENNA

3.1. Optimization Parameters and Goals

The goal of the optimization procedure is to operate with maximum gain and minimum reflection coefficient at a band of frequencies (1.2 to 6.65 GHz, 50 Ohm input impedance for a 50 Ohm feeding transmission line, depending on the values of the varactor diodes).

As already mentioned, optimization parameters include the height (h) and width (W) of R-PIFA, and the reactive load values of the passive elements. However, each shorting pin is independently loaded; therefore, all three reactance values of the passive elements participate in the optimization procedure. The optimization parameters are tabulated in Table 1 further below. One GA firstly run to optimize the dimensions of the antenna at the central frequency of 1.8 GHz. Afterwards numerous GA's run to optimize the impedance matching in any frequency between the 1 GHz–3 GHz (Table 2).

3.2. Objective Function of the First GA

The objective function (Of) deployed to obtain desired input impedance level is expressed as:

$$Of = (VSWR_{DES}/VSWR)^2$$

where $VSWR_{DES}$, $VSWR$ are the desired and computed values, respectively [17, 18]. The constraint of $VSWR_{DES}$ was set equal to 1. The simulation frequency of the **first** GA was set to 1800 MHz. The total population consists of 250 generations with 60 chromosomes per generation. The selection method was population decimation, while adjacent fitness pairing was the mating scheme. The crossover point was chosen randomly, and each chromosome was divided at a gene level. The mutation probability was equal to 0.15 [17–20]. As previously stated, Table 1 describes the variation of the parameters that took part in the GA optimization procedure. The proposed antenna dimensions are expressed in terms of the number of segments. Each segment length was selected to be equal to segment length = $0.025 * \lambda$. The results of the optimization implementation are exhibited in Table 1. The desired impedance bandwidth is determined by the band of frequencies where the value of the reflection coefficient at the feed point is less than -10 dB, corresponding to a VSWR with a value of no more than 2, when a characteristic impedance of 50Ω is considered.

Table 1. Input parameters and results of the GA for the antenna at central freq. of 1.8 GHz ($\lambda_0 = 16,655$ cm) and variation of the load reactance of the sorting pins.

Parameter	Variation	Step	GA Results	Physical Dimensions
Length of the upper plate (upLen)	$0.025 * \lambda_o - 0.25 * \lambda_o$	$0.025 * \lambda_o$	$0.125 * \lambda_o$	2.08 cm
Width of the upper plate (upWid)	$0.025 * \lambda_o - 0.25 * \lambda_o$	$0.025 * \lambda_o$	$0.125 * \lambda_o$	2.08 cm
Length of ground plane	$0.125 * \lambda_o - 0.75 * \lambda_o$	$0.025 * \lambda_o$	$0.325 * \lambda_o$	5.41 cm
Width of ground plane	$0.125 * \lambda_o - 0.75 * \lambda_o$	$0.025 * \lambda_o$	$0.275 * \lambda_o$	4.58 cm
Height of wires/shorting strips	$0.025 * \lambda_o - 0.125 * \lambda_o$	$0.025 * \lambda_o$	$0.05 * \lambda_o$	0.83 cm
			1.8 GHz	
Load reactance of the 1st parasitic element (X_1)	$-353j : 111j \Omega$	$10j \Omega$	$-150j \Omega$	
Load reactance of the 2nd parasitic element (X_2)	$-353j : 111j \Omega$	$10j \Omega$	$-60j \Omega$	
Load reactance of the 3rd parasitic element (X_3)	$-353j : 111j \Omega$	$10j \Omega$	$-90j \Omega$	

Table 2. Results of the GAs for the patch antenna with respect to the frequency and the load reactance of the sorting pins.

Frequency in MHz	Load reactance of the 1st parasitic element (X_1)	Load reactance of the 2nd parasitic element (X_2)	Load reactance of the 3rd parasitic element (X_3)	VSWR parameter
1200	-57	-124	-115	2,2371
1300	-264	-72	-77	1,6837
1400	-69	110	-118	2,0293
1500	96	-120	-56	1,0846
1600	-76	110	-147	1,4359
1700	-76	-5	-154	1,6647
1800	-164	-91	-125	1,0701
1900	86	-105	-127	1,1367
2000	-84	82	-231	1,0677
2100	-84	-5	-236	1,0336
2200	-62	-109	-176	1,0111
2300	-247	-72	-65	1,0069
2400	-256	-89	-34	1,0093
2500	-62	-74	-319	1,0495
2600	-286	-135	-238	1,0146
2700	-215	-160	-214	1,3768
2800	-293	-153	-282	1,113
2900	-293	-167	-291	1,3696
3000	-336	-174	-327	1,4861
3100	81	68	11	1,12888
3200	96	39	0	1,2312
3300	94	3	11	1,2830
3400	109	-26	11	1,3604
3500	81	-73	102	1,3561
3600	-5	-33	68	1,64
3700	53	-62	24	1,6606
3800	98	-120	81	1,6941
3900	110	-148	110	1,7284
4000	104	-163	107	1,8191
4100	98	-177	96	1,9037
4200	100	-202	108	1,9775
4300	52	-203	91	2,0516
4400	24	-192	53	2,1244
4500	46	-228	50	2,1431
4600	53	-270	60	2,1657
4700	39	-293	53	2,1786
4800	7	-278	24	2,1734
4900	-4	-278	-5	2,1552
5000	-17	-306	-7	2,1168
5100	-35	-316	-19	2,068
5200	-51	-304	-41	2,0064

Frequency in MHz	Load reactance of the 1st parasitic element (X_1)	Load reactance of the 2nd parasitic element (X_2)	Load reactance of the 3rd parasitic element (X_3)	VSWR parameter
5300	-62	-305	-59	1,9353
5400	-92	-293	-68	1,856
5500	-113	-250	-88	1,7713
5600	-127	-221	-111	1,6858
5700	-147	-172	-135	1,6043
5800	-163	-153	-156	1,5308
5900	-192	-120	-173	1,4654
6000	-214	-120	-192	1,4226
6100	-233	-59	-236	1,3883
6200	-293	-120	-217	1,4223
6300	-303	-4	-300	1,3901
6400	-339	-4	-329	1,4057
6500	-350	-120	-329	1,591
6600	-350	-120	-350	1,7586

As previously mentioned, the scope of the paper is to design a reconfigurable antenna capable to operate in a band of frequencies appropriate for microwave radiometry. Therefore, although the first optimization of the proposed antenna ran for the central resonant frequency of 1.8 GHz, a lot of GA took place afterwards with the same demands in order to calculate only the values of the reactive loads of the parasitic elements (X_1 , X_2 , X_3) separately for a band of other frequencies (from 1.2 GHz to 6.65 GHz, with a step of 10 MHz) while keeping all the other parameters constant. In that way we can change the resonant frequency by only controlling the values of the reactive loads of the shorting pins while keeping the geometry and physical size of the antenna constant. The result of these GA's is exhibited in Table 2 (step of 100 MHz).

4. NUMERICAL RESULTS

Two sets of Genetic Algorithms optimization routines ran, one to optimize the structure (size, VSWR, radiation Pattern) at the central frequency of 1.8 GHz, and the other is a set of numerous GA algorithm procedures (one for each resonant frequency and the VSWR parameter for that range depicted in the Figure 8) with all the parameters constant (taken from the first GA) except for the 3 values of the load reactance of the parasitic elements. The result of the second set of GA's is depicted in Table 2.

Table 1 describes the variation of the parameters that took part in the GA optimization procedure at the central frequency of 1.8 GHz, and the respective radiation patterns is depicted in Figures 9, 10

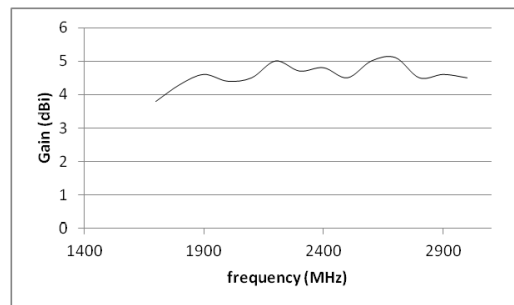


Figure 7. Peak gain variation of the proposed patch antenna calculated by SNEC software in a range of frequencies from 1.5–3 GHz.

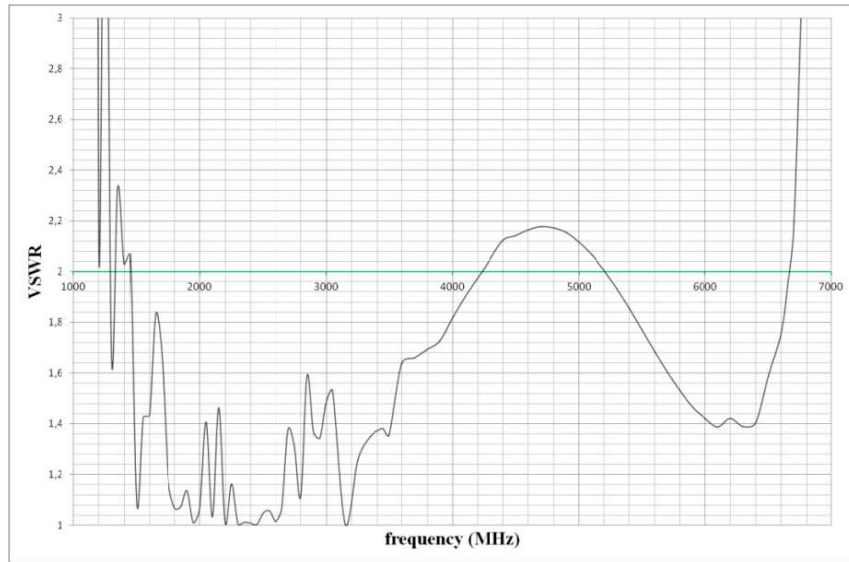


Figure 8. The SWR parameter of the optimized array in the frequency band of 1.2–6.65 GHz.

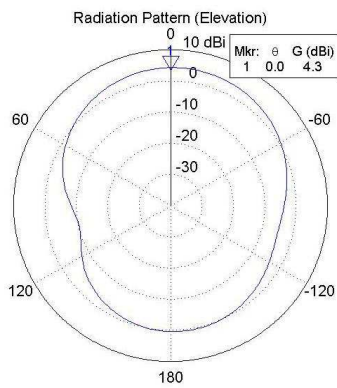


Figure 9. Radiation pattern of the optimized antenna at 1.8 GHz in the xz plane (elevation) from the SNEC.

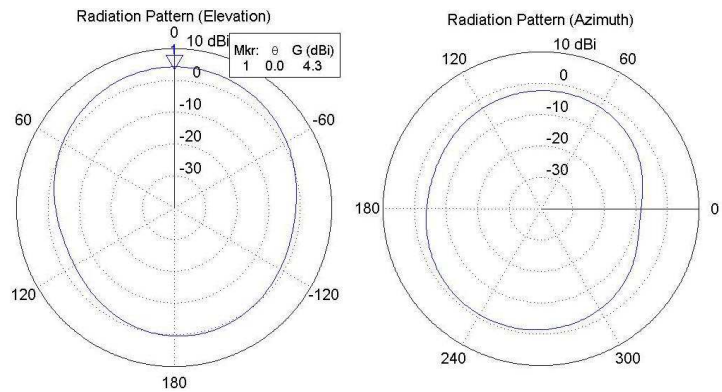


Figure 10. Radiation pattern of the optimized antenna at 1.8 GHz in the yz plane (elevation), and xy plane (azimuth) from the SNEC.

and 11. The proposed array dimensions are expressed in terms of the number of wavelength and in cm. Each segment length was selected equal to 0.025λ . The results of the optimization are exhibited also in Table 1. In Figure 7, the variation of gain in the frequency range of 1.5 to 3 GHz is plotted indicating that the gain remains almost constant in the frequency range of interest.

Figure 4(b) and Figure 5 demonstrate implementation of the proposed antenna using capacitors (static values $X_1 = -62$, $X_2 = -28$, $X_3 = -94$) instead of varactor diodes (convenience to fabricate a prototype) tuning in the central frequency of 1250 MHz showing the consistency between the simulation results and the physical structure measurement.

As shown in Figure 8, the optimized antenna can exhibit impedance matching at any frequency between 1.2 and 6.65 GHz (according to the values of the load reactance of the parasitic elements) and the values exhibited in Table 2 for the correspondent frequencies from 1.2 to 6.6 GHz with a step of 100 MHz. Also, in Figure 9 and Figure 10, it is depicted that the simulated structure demonstrates a main beam towards 90° (elevation), with a 3dB-beamwidth of 100° , a gain of 4–5 dB and in the azimuth is almost omnidirectional, as confirmed with the HFSS in Figure 11. It should be noted that these values are maintained through the entire range of **4 GHz** operating bandwidth of the proposed structure, thus making the achieved beamwidth and gain quite satisfactory.

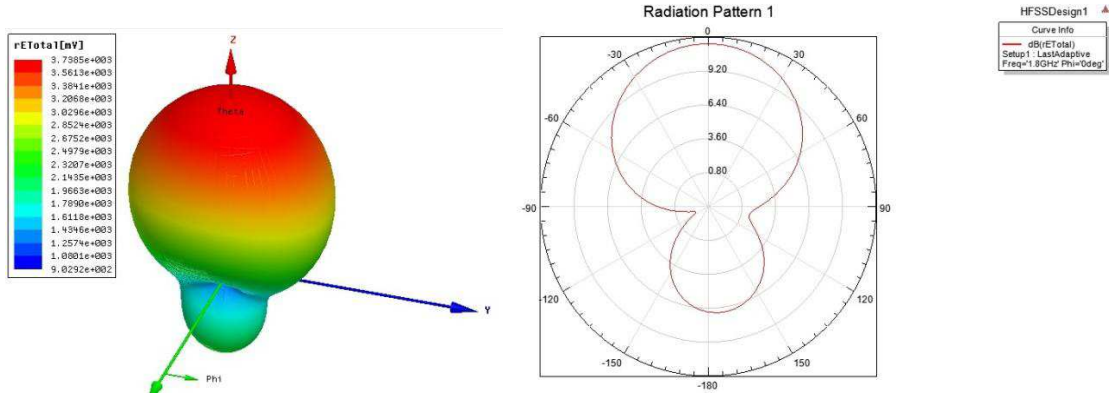


Figure 11. A 2D and 3D Radiation pattern of the optimized antenna at 1.8 GHz using HFSS (elevation).

5. CONCLUSION

A low-profile small reconfigurable patch antenna was presented in this paper to add new perspectives in the front end (antenna part) of a single channel microwave radiometer offering wider frequency range and detailed frequency tuning (in **any** central frequency, with a 40–80 MHz bandwidth) compared to tunable/reconfigurable antennas (and to previous work of the authors), without having an ultra-wideband performance. The operational bandwidth performance was optimized using the technique of the genetic algorithms and the tuning of the resonant frequency achieved by controlling the values of the varactor diodes while the central aim in design was to receive microwave signals in the frequency region of few GHz (1.2 to 6.6 GHz). The referred dynamic tuning range for the band of frequencies is 293%, and from the authors' knowledge there is no similar structure capable to achieve these goals in such wide range. The in-band maximum gain is around 4–5 dB throughout the microwave radiometer spectrum. In this paper, the characteristics of a single element antenna were studied and analyzed while a reconfigurable range of 4 GHz is archived appropriately for use as the antenna part of a single-channel microwave radiometer.

REFERENCES

1. Sprawls, P., *Physical Principles of Medical Imaging*, Lippincott Williams and Wilkins, 1987.
2. Nikawa, Y., M. Chino, and K. Kikuchi, "Soft and dry phantom modeling material using silicone rubber with carbon fibre," *IEEE Trans. Microw. Theory Tech.*, Vol. 44, No. 10, 1949–1953, 1996.
3. Lagendijk, J. J. W. and P. Nilsson, "Hyperthermia dough: A fat and bone equivalent phantom to test microwave/radiofrequency hyperthermia heating systems," *Phys. Med. Biol.*, Vol. 30, No. 7, 709–712, 1985.
4. Preece, A. W., J. L. Green, N. Potheary, and R. H. Johnson, "Microwave imaging for tumour detection," *IEE Colloquium on Radar and Microwave Imaging*, 9/1–9/4, The Institution of Electrical Engineers, Savoy Place, London WC2R OBL, UK, 1994.
5. Pozar, D. M., *Microwave Engineering*, 3rd Edition, John Wiley and Sons, 2004.
6. Gabriel, S., R. W. Lau, and C. Gabriel, "The dielectric properties of biological tissues: III. Parametric models for the dielectric spectrum of tissues," *Physics in Medicine and Biology*, Vol. 41, No. 11, 2271–2293, 1996.
7. IFAC, "An internet resource for the calculation of the dielectric properties of body tissues," *Italian National Research Council Institute for Applied Physics*, Sep. 2011.
8. Hurt, W. D., "Multiterm debye dispersion relations for permittivity of muscle," *IEEE Transactions on Biomedical Engineering*, Vol. 32, No. 1, 60–64, Jan. 1985.
9. Cole, K. S. and R. H. Cole, "Dispersion and absorption in dielectrics. I. Alternating current characteristics," *Journal Chem. Phys.*, Vol. 9, 341–351, 1941.

10. Paulides, M. M., J. F. Bakker, N. Chavannes, and G. C. Van Rhoon, "A patch antenna design for application in a phased-array head and neck hyperthermia applicator," *IEEE Transactions on Biomedical Engineering*, Vol. 54, No. 11, 2057–2063, Nov. 2007.
11. Gabriel, C., S. Gabriely, and E. Corthout, "The dielectric properties of biological tissues: I. Literature survey," *Phys. Med. Biol.*, Vol. 41, 2231–2249, 1996.
12. Miklavcic, D., N. Pavselj, and F. X. Hart, "Electric properties of tissues," *Wiley Encyclopedia of Biomedical Engineering*, John Wiley & Sons, Inc., Copyright, 2006.
13. Nikolopoulos, C. D. and C. N. Capsalis, "A novel antenna system for body temperature change detection appropriate for multi-channel microwave radiometry," *Progress In Electromagnetics Research M*, Vol. 33, 197–209, 2013.
14. Liang, J. and H. Y. D. Yang, "Varactor loaded tunable printed PIFA," *Progress In Electromagnetics Research B*, Vol. 15, 113–131, 2009.
15. El-Sharkawy, A. M., P. P. Sotiriadis, P. A. Bottomley, and E. Atalar, "A new RF radiometer for absolute noninvasive temperature sensing in biomedical applications," *IEEE International Symposium on Circuits and Systems, ISCAS 2007*, 329–332, 2007.
16. Curto, S., P. McEvoy, X. Bao, and M. J. Ammann, "Compact patch antenna for electromagnetic interaction with human tissue at 434 MHz," *IEEE Transactions on Antennas and Propagation*, Vol. 57, No. 9, 2564–2571, Sep. 2009.
17. Goldberg, D. E., *Genetic Algorithms in Search, Optimization, and Machine Learning*, Addison-Wesley Publishing Company, Inc., 1989.
18. "SuperNec v. 2.4 MOM technical reference manual," Available at: <http://www.supernec.com/manuals/snmomtrm.htm>.
19. Fourie, A. and D. Nitch, "SuperNEC: Antenna and indoor-propagation simulation program," *IEEE Antennas and Propagat. Mag.*, Vol. 42, No. 3, 31–48, Jun. 2000.
20. Rahmat-Samii, Y. and E. Michielssen, *Electromagnetic Optimization by Genetic Algorithms*, John Wiley & Sons, Inc., 1999.